Inorg. Chem. **2006**, *45*, 10990–10997

Inorganic Chemistry
Article

Dinuclear Iridium(III) Complexes Consisting of Back-to-Back tpy–(ph)$_n$–tpy Bridging Ligands ($n = 0$, 1, or 2) and Terminal Cyclometallating Tridentate N–C–N Ligands

Audrey Auffrant,[†] Andrea Barbieri,[‡] Francesco Barigelletti,*[,‡] Jean-Paul Collin,*[,†] Lucia Flamigni,[‡] Cristiana Sabatini,[‡] and Jean-Pierre Sauvage[†]

Laboratoire de Chimie Organo-Minérale, UMR 7513 du CNRS, Institut Le Bel, Université Louis Pasteur, 4 rue Blaise Pascal, 67000 Strasbourg Cedex, France, and Istituto per la Sintesi Organica e la Fotoreattività (ISOF), Consiglio Nazionale delle Ricerche (CNR), Via P. Gobetti 101, 40129 Bologna, Italy

Received June 7, 2006

Three dinuclear iridium(III) complexes consisting of a conjugated bis-tpy type bridging ligand and cyclometallating capping tridentate ligands of the 1,3-di-2-pyridylbenzene family have been prepared (tpy, 2,2′,6′,2′′-terpyridine). The two tpy units of the bridge are connected via their back-positions (4′) either directly or with a *p*-phenylene or *p*-biphenylene spacer. The synthesis relies on the reaction between the dinuclear $[Ir(dpb)Cl_2]_2$ complex (dpb-H = 1,3-dipyridyl-4,6-dimethylbenzene) and the corresponding bis-tpy ligand. Electrochemical measurements afford metal-centered oxidation and ligand-centered reduction potentials; from the oxidation steps, no evidence is obtained for a strong coupling between the two iridium(III) subunits of the dinuclear species. For all complexes, ground-state absorption data in the 380 nm to visible region show a trend which is consistent with the presence of charge-transfer (CT) transitions involving different degrees of electronic delocalization at the bridging ligands. (dpb)Ir(tpy–tpy)Ir(dpb)$^{4+}$ exhibits an appreciable luminescence at room temperature ($\phi = 3.0 \times 10^{-3}$; $\tau = 3.3$ ns), whereas no emission from the other binuclear complexes is detected. All binuclear complexes luminesce at 77 K, and a metal-to-ligand CT nature for (dpb)Ir(tpy–tpy)Ir(dpb)$^{4+}$ is suggested, whereas a ligand-centered (LC) emission is proposed for (dpb)Ir(tpy–(ph)$_2$–tpy)Ir(dpb)$^{4+}$ on the basis of the comparison with the phosphorescence properties of the free bridging ligand, tpy–(ph)$_2$–tpy. Transient absorbance experiments at room temperature afford the absorption spectra and lifetimes of the nonemissive excited states. For (dpb)Ir(tpy–ph–tpy)Ir(dpb)$^{4+}$ and (dpb)Ir(tpy–(ph)$_2$–tpy)Ir(dpb)$^{4+}$, the spectra exhibit a broad profile peaking around 780 nm, quite intense in the case of (dpb)Ir(tpy–(ph)$_2$–tpy)Ir(dpb)$^{4+}$, and lifetimes of 160 and 440 ps, respectively.

Introduction

Dinuclear complexes of the type M−L−M′, with various bridging ligands L ensuring electronic coupling between the metal centers, have been the subject of numerous studies, in relation to photochemical energy and electron transfer,[1] mixed-valence complexes,[2] and molecular materials for electronic applications.[3] In this context, bis-tpy ligands (tpy, 2,2′,6′,2′′-terpyridine) containing two tpy units attached back-to-back (via their 4′ positions) are of particular interest since they allow good control over the geometrical properties of the system and, in particular, over the M···M′ distance.[4] In the course of the past 15 years, several groups have synthesized and investigated such complexes in detail, in

---

* To whom correspondence should be addressed. E-mail: franz@isof.cnr.it (F.B.); jpcollin@chimie.u-strasbg.fr (J.-P.C.).

[†] Université Louis Pasteur.

[‡] ISOF−CNR.

(1) (a) Balzani, V.; Scandola, F. *Supramolecular Photochemistry*; Ellis Horwood: Chichester, U.K., 1991. (b) Balzani, V.; Juris, A.; Venturi, M.; Campagna, S.; Serroni, S. *Chem. Rev.* **1996**, *96*, 759. (c) Juris, A.; Balzani, V.; Barigelletti, F.; Campagna, S.; Belser, P.; Von, Zelewsky, A. *Coord. Chem. Rev.* **1988**, *84*, 85.

(2) Demadis, K. D.; Hartshorn, C. M.; Meyer, T. J. *Chem. Rev.* **2001**, *101*, 2655.

(3) Welter, S.; Brunner, K.; Hofstraat, J. W.; De Cola, L. *Nature* **2003**, *421*, 54.

(4) (a) Sauvage, J.-P.; Collin, J.-P.; Chambron, J.-C.; Guillerez, S.; Coudret, C.; Balzani, V.; Barigelletti, F.; De, Cola, L.; Flamigni, L. *Chem. Rev.* **1994**, *94*, 993. (b) Barigelletti, F.; Flamigni, L. *Chem. Soc. Rev.* **2000**, *29*, 1.

10.1021/ic061009q CCC: $33.50

particular with M = Ru(II) and M′ = Os(II) [5] or Rh(III),[6] showing that the electron- or energy-transfer rates between the electron or energy donor part (Ru(II)) and the electron (Rh(III)) or energy (Os(II)) acceptor component can be tuned by controlling the length and the nature of the bridge. Symmetrical tpy complexes of the M−L−M family (M = Ru(II))[7] or their cyclometalating analogues[8] display interesting electronic and photochemical properties, distinctly different from their mononuclear parent complexes. Ir(III) tpy complexes are also interesting candidates to be incorporated in such dinuclear complexes since $Ir(tpy)_2^{3+}$ and its derivatives are luminescent species with a long-lived excited state and a high excited-state energy content.[9]

In the present paper, we describe the synthesis and the redox and photochemical properties of symmetrical species of the Ir−L−Ir family. Cyclometalating Ir(III) complexes, mostly containing bidentate cyclometalating ligands, have recently been much investigated as highly luminescent molecular species to be used as chromophores in the fabrication of organic light-emitting diodes.[10] Recently, Williams et al. have reported the preparation and the photochemical properties of a neutral mononuclear iridium(III) complex containing two cyclometalating terdentate ligands reminiscent of tpy.[11] We anticipated that the incorporation of related cyclometalating tridentate compounds into dinuclear Ir−L−Ir compounds with bridging bis-tpy ligands would lead to new electronic properties, both as mixed valence species and in relation to their photochemical and photophysical characteristics. In particular, the present report shows that the smallest dinuclear species displays interesting excited-state properties, with a weak but noticeable luminescence at room temperature which is not found in the mononuclear precursor.

Scheme 1. Chemical Formulas of the Ligands and Complexes Synthesized

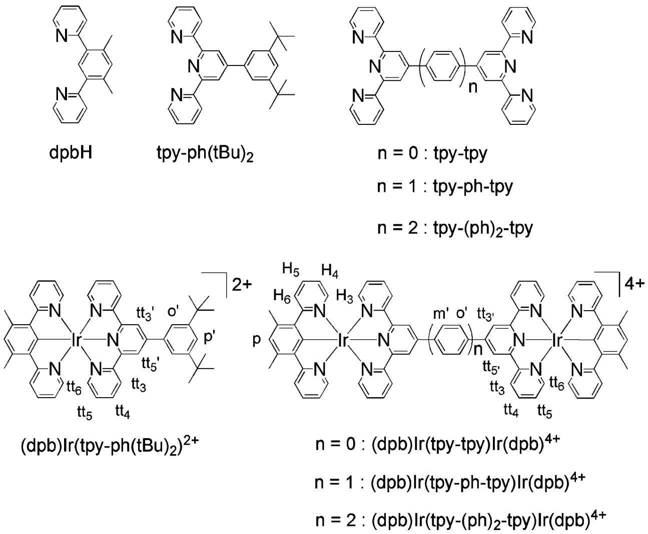

Scheme 2. Synthesis of the Mono- and Dinuclear Iridium(III) Complexes

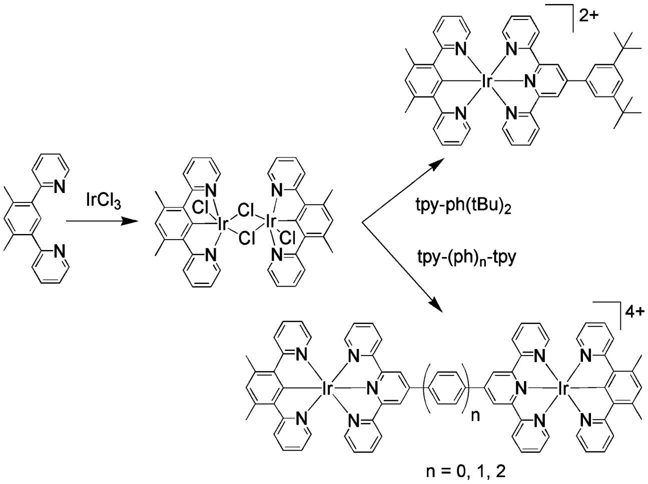

Results and Discussion

Syntheses. The ligands and iridium complexes involved in this study are represented in Scheme 1. The ligands 1,3-dipyridyl-4,6-dimethylbenzene (dpb-H),[12] (4′-(3,5-di-*tert*-butylbenzene)-2,2′:6′,2″-terpyridine[9a] (tpy-ph(tBu)$_2$), tpy−tpy,[13] tpy−ph−tpy,[14] and tpy−(ph)$_2$−tpy [15] have been

---

(5) (a) Barigelletti, F.; Flamigni, L.; Balzani, V.; Collin, J.-P.; Sauvage, J.-P; Sour, A.; Constable, E. C.; Thompson, A. M. W. C. *J. Am. Chem. Soc.* **1994**, *116*, 7692. (b) Grosshenny, V.; Harriman, A.; Ziessel, R. *Angew. Chem., Int. Ed. Engl.* **1995**, *34*, 1100. (c) Hammarstroem, L.; Barigelletti, F.; Flamigni, L.; Armaroli, N.; Sour, A.; Collin, J.-P.; Sauvage, J.-P. *J. Am. Chem. Soc.* **1996**, *118*, 11972.(d) Harriman, A.; Khatyr, A.; Ziessel, R.; Benniston, A. C. *Angew. Chem., Int. Ed.* **2000**, *39*, 4287. (e) Encinas, S.; Flamigni, L.; Barigelletti, F.; Constable, E. C.; Housecroft, C. E.; Schofield, E. R.; Figgemeier, E.; Fenske, D.; Neuburger, Ma.; Vos, J. G.; Zehnder, M. *Chem. Eur. J.* **2002**, *8*, 137. (f) Akasaka, T.; Otsuki, J.; Araki, K. *Chem. Eur. J.* **2002**, *8*, 130.

(6) (a) Indelli, M. T.; Scandola, F.; Collin, J.-P.; Sauvage, J.-P.; Sour, A. *Inorg. Chem.* **1996**, *35*, 303. (b) Lee, J.-D.; Vrana, L. M.; Bullock, E. R.; Brewer, K. J. *Inorg. Chem.* **1998**, *37*, 3575. (c) Yutaka, T.; Mori, I.; Kurihara, M.; Mizutani, J.; Kubo, K.; Furusho, S.; Matsumura, K.; Tamai, N.; Nishihara, H. *Inorg. Chem.* **2001**, *40*, 4986.

(7) (a) Hammarström, L.; Barigelletti, F.; Flamigni, L.; Indelli, M. T.; Armaroli, N.; Calogero, G.; Guardigli, M.; Sour, A.; Collin, J.-P.; Sauvage, J.-P. *J. Phys. Chem. A* **1997**, *101*, 9061. (b) Barbieri, A.; Ventura, B.; Barigelletti, F.; De Nicola, A.; Quesada, M.; Ziessel, R. *Inorg. Chem.* **2004**, *43*, 7359.

(8) (a) Beley, M.; Collin, J.- P.; Louis, R.; Metz, B.; Sauvage, J.-P. *J. Am. Chem. Soc.* **1991**, *113*, 8521. (b) Beley, M.; Chodorowski, S.; Collin, J.-P.; Sauvage, J.-P.; Flamigni, L.; Barigelletti, F. *Inorg. Chem.* **1994**, *33*, 2543. (c) Sutter, J.-P.; Grove, D. M.; Beley, M.; Collin, J.-P.; Veldman, N.; Spek, A. L.; Sauvage, J.-P.; van Koten, G. *Angew. Chem.* **1994**, *106*, 1359. (d) Beley, M.; Chodorowski-Kimmes, S.; Collin, J.-P.; Laine, P.; Launay, J.-P.; Sauvage, J.-P. *Angew. Chem.* **1994**, *106*, 1854. (e) Patoux, C.; Launay, J.-P.; Beley, M.; Chodorowski-Kimmes, Sa.; Collin, J.-P.; James, S.; Sauvage, J.-P. *J. Am. Chem. Soc.* **1998**, *120*, 3717. (f) Barigelletti, F.; Flamigni, L.; Collin, J.-P.; Sauvage, J.-P. *Chem. Commun.* **1997**, *4*, 333.

(9) (a) Collin, J.-P.; Dixon, I. M.; Sauvage, J.-P.; Williams, J. A. G.; Barigelletti, F.; Flamigni, L. *J. Am. Chem. Soc.* **1999**, *121*, 5009. (b) Dixon, I.; Collin, J.-P.; Sauvage, J.-P.; Barigelletti, F.; Flamigni, L. *Angew. Chem., Int. Ed.* **2000**, *39*, 1292. (c) Baranoff, E.; Dixon, I.; Collin, J.-P.; Sauvage, J.-P.; Ventura, B.; Flamigni, L. *Inorg. Chem.* **2004**, *43*, 3057.

(10) (a) Lamansky, S.; Djurovich, P.; Murphy, D. Abdel-Razzaq, F.; Lee, H.-E.; Adachi, C.; Burrows, P. E.; Forrest S. R.; Thompson, M. E. *J. Am. Chem. Soc.* **2001**, *123*, 4304. (b) Lo, S.-C.; Male, N. A.; Markham, J. P. J.; Magennis, S. W.; Burn, P. L.; Salata, O. V; Samuel, I. D. *Adv. Mater.* **2002**, *14*, 975. (c) Nam, E. J.; Kim J. H; Kim B.-O.; Kim, S. M.; Park, N. G.; Kim Y. S.; Kim, Y. K.; Ha, Y. *Bull. Chem. Soc. Jpn.* **2004**, *77*, 751. (d) Grushin, V. V.; Herron, N.; LeCloux, D. D.; Marshall, W. J.; Petrov, V. A.; Wang, P.Y. *Chem. Commun.* **2001**, 1494.

(11) (a) Wilkinson, A. J.; Goeta, A. E.; Foster, C. E.; Williams, J. A. G. *Inorg. Chem.* **2004**, *43*, 6513. (b) Bexon, A. J. S.; Williams, J. A. G. *C. R. Acad. Sci., Ser. IIc: Chim.* **2005**, *8*, 1326.

(12) Cardenas, D. J.; Echavarren, A. M. *Organometallics* **1999**, *18*, 3337.

(13) Constable, E.C.; Ward, M.D. *J. Chem. Soc., Dalton Trans.* **1990**, 1405.

Table 1. Electrochemical Data for Mono- and Dinuclear Iridium Complexes

complex	Ir^{IV}/Ir^{III} (ΔE_p, mV)	L/L^- (ΔE_p, mV)	L^-/L^{2-}
$(dpb)Ir(tpy{-}ph(tBu)_2)^{2+}$	1.78 (70)[a]	−0.99 (60)[a]	−1.45 (irrev)[a]
$(dpb)Ir(tpy{-}tpy)Ir(dpb)^{4+}$	1.76 (80)[b]	−0.68 (60),[a] −0.95 (60)[a]	−1.54 (irrev)[b]
$(dpb)Ir(tpy{-}ph{-}tpy)Ir(dpb)^{4+}$	1.76 (90)[b]	−0.97 (70)[b]	−1.45 (irrev)[b]
$(dpb)Ir(tpy{-}(ph)_2{-}tpy)Ir(dpb)^{4+}$	1.74 (90)[b]	−0.99 (70)[b]	−1.43 (irrev)[b]

[a] Monoelectronic wave. [b] Bielectronic wave.

synthesized as previously described. The cyclometallated iridium starting dimer $[Ir(dpb)Cl_2]_2$ was prepared in 60% yield by heating a solution of $IrCl_3$ and dpbH in 2-ethoxyethanol.[11a]

The reaction of $[Ir(dpb)Cl_2]_2$ and bis-terpyridine tpy−tpy, tpy−ph−tpy, and $tpy{-}(ph)_2{-}tpy$ in ethylene glycol at reflux gave access to the desired complexes (obtained as PF_6^- salts), incorporating a bis-terpyridine linker and the cyclometallated dpb ligand in 50, 26, and 25% yield, respectively (Scheme 2). For the sake of comparison the monomer $(dpb)Ir(tpy{-}ph(tBu)_2)(PF_6)_2$ was also prepared in the same manner in 55% yield. Because of the inertness of the coordination sphere of the Ir(III) atom, these syntheses require harsh conditions with a strict control of the reaction time. Several byproducts are also obtained, and some carefully conducted chromatography columns are necessary to achieve purification. This explains the observed moderate to low yields range.

Particular attention has been brought to the purification of all the iridium complexes. They have been systematically submitted to silica gel chromatography eluted with a mixture of high-purity polar solvents (CH_3CN−aqueous KNO_3 solution) and characterized by thin-layer chromatography, UV−visible electronic spectroscopy, cyclic voltammetry, ^1H and ^{13}C NMR, and high-resolution mass spectroscopy.

Electrochemistry. The electrochemical properties of the cyclometalated iridium complexes were examined by cyclic voltammetry in acetonitrile at room temperature. The redox potentials measured relative to SCE are reported in Table 1.

For the mononuclear complex $(dpb)Ir(tpy{-}ph(tBu)_2)^{2+}$, a reversible one-electron oxidation wave was observed at 1.78 V. This relatively low oxidation potential value reflects the strong σ-donor ability of the 1,3-dipyridyl-4,6-dimethylbenzene anionic ligand. It is, to our knowledge, the first monocyclometalating ligand that increases sufficiently the electronic density at the metal center to observe the Ir^{IV}/Ir^{III} redox couple in a conventional potential window. A reversible two-electron oxidation process around 1.76 V was also observed for the three dinuclear iridium complexes. Several reports in the literature indicate that these processes are due to removal of metal-localized electrons,[16−18] although density functional theory (DFT) calculations show that in some cases the HOMOs may be partially delocalized over the iridium−aryl fragment.[19,20] At negative potentials, the complex $(dpb)Ir(tpy{-}ph(tBu)2)^{2+}$ exhibits a reversible one-electron process at −0.99 V and an irreversible process at −1.45 V. A similar pattern is observed in the case of the dinuclear complexes (n = 1 or 2), but each wave corresponds to a two-electron process. By comparison with related complexes,[8b,21] these processes can be assigned to the reduction of the central bis-terpyridine ligand. In the case of $(dpb)Ir(tpy{-}tpy)Ir(dpb)^{4+}$, two reversible monoelectronic waves are observed at −0.68 and −0.95 V and a third one at −1.54 V. The splitting of the first reduction processes on the central bis-terpyridine in two waves separated by 270 mV is an indication of a significant delocalization occurring in this dinuclear complex.

Electronic Spectroscopy. Ground-State Absorption. Figure 1 shows the absorption spectra for the complexes and the ligands of Scheme 1, as obtained in acetonitrile and dichloromethane solutions, respectively. Absorption data are collected in Table 2. For mononuclear complex $(dpb)Ir(tpy{-}ph(tBu)_2)^{2+}$, a strong UV absorption is found in the region of 280−320 nm ($\epsilon \sim 5 \times 10^4$ M^{-1} cm^{-1}), which is ascribable to intraligand ^1LC (LC = ligand-centered) transitions.[22−28] At lower energies, a less intense absorption region with onset at 400 nm is also found ($\epsilon \sim 2 \times 10^4$ M^{-1} cm^{-1}), with an even weaker one in the region of 400−500 nm. For the former, peaking at 373 nm, either Ir→tpy (^1MLCT) or dpb→tpy (^1LLCT)[20,29] transitions could be involved. For the tail extending at $\lambda > 400$ nm ($\epsilon_{440} = 1400$ M^{-1} cm^{-1}), and due to the heavy-atom effect (as it happens for Os(II) complexes containing tpy and bpy ligands),[30] formally forbidden metal-to-ligand charge transfer (MLCT) or ligand-to-ligand CT (LLCT) singlet-to-triplet transitions might be called for.

---

(14) Constable, E.C.; Thompson, A. *J. Chem. Soc., Dalton Trans.* **1992**, 3467.

(15) Collin, J. P.; Lainé, P.; Launay, J.-P.; Sauvage, J.-P.; Sour, A. *J. Chem. Soc., Chem. Commun.* **1993**, 434.

(16) Ohsawa, Y.; Sprouse, S.; King, K. A.; DeArmond, M. K.; Hanck, K. W.; Watts, R. J. *J. Phys. Chem.* **1987**, *91*, 1047.

(17) Lo, K. K.-W.; Chung, C.-K.; Zhu, N. *Chem. Eur. J.* **2003**, *9*, 475.

(18) Mamo, A.; Stefio, I.; Parisi, M. F.; Credi, A.; Venturi, M.; Di Pietro, C.; Campagna, S. *Inorg. Chem.* **1997**, *36*, 5947.

(19) Tamayo, A. B.; Alleyne, B. D.; Djurovich, P. I.; Lamansky, S. Tsyba, I.; Ho, N. N.; Bau, R.; Thompson, M. E. *J. Am. Chem. Soc.* **2003**, *125*, 7377.

(20) Polson, M.; Fracasso, S.; Bertolasi, V.; Ravaglia, M.; Scandola, F. *Inorg. Chem.* **2004**, *43*, 1950.

(21) Griffiths, P. M.; Loiseau, F.; Puntoriero, F.; Serroni, S.; Campagna, S. *Chem. Commun.* **2000**, 2297.

(22) Flamigni, L.; Barigelletti, F.; Amaroli, N.; Ventura, B.; Collin, J.-P.; Dixon, I. M.; Sauvage, J.-P.; Williams, J. A. G. *Coord. Chem. Rev.* **1999**, *190−192*, 671.

(23) Licini, M.; Williams, J. A. G. *Chem. Commun.* **1999**, 1943.

(24) Goodall, W.; Williams, J. A. G. *J. Chem. Soc., Dalton Trans.* **2000**, 2893.

(25) Dixon, I. M.; Collin, J.-P.; Sauvage, J.-P.; Flamigni, L.; Encinas, S.; Barigelletti, F. *Chem. Soc. Rev.* **2000**, *29*, 385.

(26) Baranoff, E.; Collin, J.-P.; Flamigni, L.; Sauvage, J.-P. *Chem. Soc. Rev.* **2004**, *33*, 147.

(27) Lu, W.; Mi, B. X.; Chan, M. C. W.; Hui, Z.; Che, C. M.; Zhu, N. Y.; Lee, S. T. *J. Am. Chem. Soc.* **2004**, *126*, 4958.

(28) Flamigni, L.; Ventura, B.; Barigelleti, F.; Baranoff, E.; Collin, J.-P.; Sauvage J.-P. *Eur. J. Inorg. Chem.* **2005**, 1312.

(29) Polson, M.; Ravaglia, M.; Fracasso, S.; Garavelli, M.; Scandola, F. *Inorg. Chem.* **2005**, *44*, 1282.

(30) Kober, E. M.; Caspar, J. V.; Lumpkin, R. S.; Meyer, T. J. *J. Phys. Chem.* **1986**, *90*, 3722.

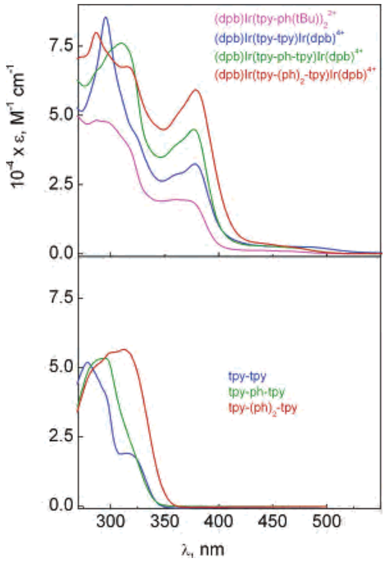

Figure 1. Ground-state absorption spectra for complexes (upper panel, acetonitrile solvent) and ligands (lower panel, dichloromethane solvent).

Table 2. Ground-State Absorption Data[a]

compound	λ_{max}, nm (ϵ, M^{-1} cm^{-1})
(dpb)Ir(tpy−ph(tBu)$_2$)$^{2+}$	264 (51 300), 373 (19 200), 440 (1400)
(dpb)Ir(tpy−tpy)Ir(dpb)$^{4+}$	295 (85 600), 378 (32 500), 490 (3000)
(dpb)Ir(tpy−ph−tpy)Ir(dpb)$^{4+}$	310 (76 200), 377 (45 000), 446 (2800)
(dpb)Ir(tpy−(ph)$_2$−tpy)Ir(dpb)$^{4+}$	287 (79 900), 379 (59 200), 441 (3800)
tpy−tpy	278 (51 900), 315 (19 000)
tpy-ph-tpy	295 (53 400)
tpy−(ph)$_2$−tpy	312 (56 400)

[a] At rt, in acetonitrile and dichloromethane solvents for the complexes and the ligands, respectively.

Regarding the binuclear complexes (dpb)Ir(tpy−tpy)Ir(dpb)$^{4+}$, (dpb)Ir(tpy−ph−tpy)Ir(dpb)$^{4+}$, and (dpb)Ir(tpy−(ph)$_2$−tpy)Ir(dpb)$^{4+}$ (Figure 1, upper panel), it is noticed that the absorption intensity for the CT band around 380 nm is (i) larger than what happens for (dpb)Ir(tpy−ph(tBu)$_2$)$^{2+}$ and (ii) increases further along the series (dpb)Ir(tpy−tpy)Ir(dpb)$^{4+}$, (dpb)Ir(tpy−ph−tpy)Ir(dpb)$^{4+}$, and (dpb)Ir(tpy−(ph)$_2$−tpy)Ir(dpb)$^{4+}$; i.e., it increases with the length of the bridging ligand. The former issue is clearly related to the nuclearity of the complexes, based on which an approximate doubling of the absorption features for the binuclear complexes is expected with respect to the mononuclear case, provided transitions of CT type (either of Ir→tpy or dpb→tpy nature) are present. However, for the binuclear cases, the steady increase of absorption intensity in the 380 nm region along with the number of phenylene units [for the series (dpb)Ir(tpy−tpy)Ir(dpb)$^{4+}$, (dpb)Ir(tpy−ph−tpy)Ir(dpb)$^{4+}$, and (dpb)Ir(tpy−(ph)$_2$−tpy)Ir(dpb)$^{4+}$] also points to electronic effects at the bridging ligand. This seems partly confirmed by the absorption features exhibited by the ligands tpy−tpy, tpy−ph−tpy, and tpy−(ph)$_2$−tpy (Figure 1, lower panel). Here, the increase in bridge length results in a systematic red shift of the lowest-lying energy band. This behavior is somewhat different from that exhibited by the complexes. For these, as noted above, the lowest-energy intense band keeps at ca. 380 nm in all cases, while increasing in intensity with the size of the complexes. The found enhancement in absorption intensity along the sequence (dpb)Ir(tpy−ph(tBu)$_2$)$^{2+}$, (dpb)Ir(tpy−tpy)Ir(dpb)$^{4+}$, (dpb)Ir(tpy−ph−tpy)Ir(dpb)$^{4+}$, and (dpb)Ir(tpy−(ph)$_2$−tpy)Ir(dpb)$^{4+}$ is consistent with the occurrence of CT transitions wherein the promoted electron involves larger and larger accepting ligands, i.e., the bridging ligands. Actually, in agreement with treatments outlined in a previous paper,[7a] the distance covered by the electron promoted from the donating center to the ligand system is expected to be linearly related to the transition dipole moment for the CT transition, $\vec{\mu}$, in turn correlated with the oscillator strength, f, and the absorption intensity of the CT band, eqs 1, where $\bar{\nu}$ is in wavenumbers and $\bar{\nu}_{abs}$ is the frequency at the absorption peak.

$$f = 4.3 \times 10^{-9} \int \epsilon(\bar{\nu})\, d\bar{\nu} \tag{1a}$$

$$|\vec{\mu}| = \left(\frac{f}{1.085 \times 10^{-5} \bar{\nu}_{abs}}\right)^{1/2} \tag{1b}$$

Use of eqs 1a,b for the absorption band around 380 nm provides $\vec{\mu} = 0.84$, 1.1, 1.29, and 1.48 e·Å for (dpb)Ir(tpy−ph(tBu)$_2$)$^{2+}$, (dpb)Ir(tpy−tpy)Ir(dbp)$^{4+}$, (dpb)Ir(tpy−ph−tpy)Ir(dpb)$^{4+}$, and (dpb)Ir(tpy−(ph)$_2$−tpy)Ir(dpb)$^{4+}$, respectively, which indicates larger and larger displacement of the charge for the CT transition along the series. It is noteworthy that, in the visible region of the spectrum, the absorption intensity of the binuclear complexes (dpb)Ir(tpy−(ph)$_2$−tpy)Ir(dpb)$^{4+}$ ($\epsilon_{441} = 3800$ M^{-1} cm^{-1}) and (dpb)Ir(tpy−ph−tpy)Ir(dpb)$^{4+}$ ($\epsilon_{446} = 2800$ M^{-1} cm^{-1}) is twice in intensity as that of the mononuclear (dpb)Ir(tpy−ph(tBu)$_2$)$^{2+}$ ($\epsilon_{440} = 1400$ M^{-1} cm^{-1}); see Table 2. At odds with this, for the dinuclear complex (dpb)Ir(tpy−tpy)Ir(dpb)$^{4+}$ the band maximum is registered at lower energy (490 nm, $\epsilon = 3000$ M^{-1} cm^{-1}). This suggests that for the larger binuclear complexes the two tpy moieties of the bridging ligand are somewhat decoupled by the interposed phenylene units, whereas for (dpb)Ir(tpy−tpy)Ir(dpb)$^{4+}$ an effective delocalization is present within the back-to-back bis-tpy ligand. The occurrence of such electronic effects was previously reported for a similar series of tpy−(ph)$_{n-}$tpy-bridged Ru(II)-based binuclear species ($n = 0-2$).[7a] All of this is therefore consistent with some CT character for the (forbidden) transitions falling in the visible region.

Luminescence. Luminescence data obtained at 295 K and at 77 K are collected in Table 3; the solvents employed were acetonitrile and dichloromethane, for the complexes and the ligands, respectively.

Figure 2 shows the luminescence spectra for the complexes, as registered at room temperature and at 77 K; λ_{exc} was 380 nm. Figure 3 depicts luminescence results for the ligands with the fluorescence spectra taken at room temperature and the phosphorescence spectra registered at 77 K; λ_{exc} was 315 nm.

Among the dinuclear species, only (dpb)Ir(tpy−tpy)Ir(dpb)$^{4+}$ exhibits an appreciable luminescence at room temperature ($\phi = 3.0 \times 10^{-3}$, $\tau = 3.3$ ns; Table 3 and Figure 2, upper panel), with the emission level being the lowest-lying in energy (as also seen from the 77 K results, vide infra). This is apparently due to a larger stabilization of the LUMO

Table 3. Luminescence and Photophysical Properties[a]

compound	295 K λ_{max}, nm	ϕ	τ, ns	k_r,[b] s^{-1}	77 K λ_{max}, nm	τ
$(dpb)Ir(tpy{-}ph(tBu)_2)^{2+}$	547	3.4×10^{-4}	3.3	1.0×10^5	521	2.0 μs
$(dpb)Ir(tpy{-}tpy)Ir(dpb)^{4+}$	620	3.0×10^{-3}	6.4	4.7×10^5	565	2.2 μs
$(dpb)Ir(tpy{-}ph{-}tpy)Ir(dpb)^{4+}$	~600	c	c		532	5.6 μs [d]
$(dpb)Ir(tpy{-}(ph)_2{-}tpy)Ir(dpb)^{4+}$	~600	c	c		549	49 μs [e]
tpy−tpy	363	0.08	1.7	4.6×10^7	450[f]	1.17 s [f]
tpy−ph−tpy	360	0.13	2.2	5.9×10^7	507[f]	1.49 s [f]
$tpy{-}(ph)_2{-}tpy$	379	0.49	0.6	8.2×10^8	532[f]	1.44 s [f]

[a] In air-equilibrated acetonitrile for the complexes, λ_{exc} was 380 (intensities) and 373 nm (lifetimes). In air-equilibrated dichoromethane for the ligands, λ_{exc} was 315 (intensities) and 278 nm (lifetimes). [b] From $k_r = \phi/\tau$. [c] Too weak emission. [d] Major component (80%) of a dual exponential decay; the other τ was 1.1 μs. [e] Major component (90%) of a dual exponential decay; the other τ was 4.2 μs. [f] Results obtained by introducing a temporal delay of 100 μs to exclude detection of prompt fluorescence.

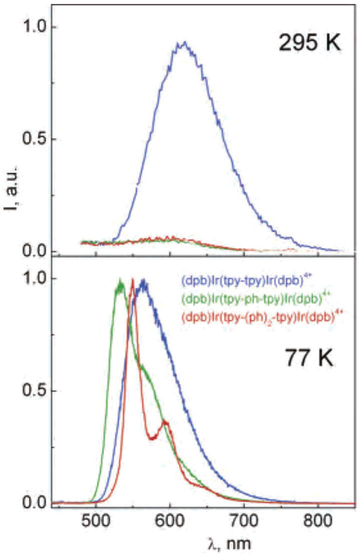

Figure 2. Luminescence spectra *i* for acetonitrile solutions of the complexes at room temperature (upper panel, isoabsorbing samples at λ_{exc} = 380 nm) and at 77 K (lower panel, normalized spectra).

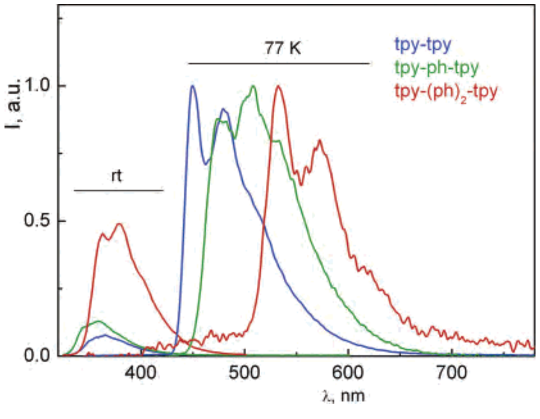

Figure 3. Luminescence spectra for the ligands in dichloromethane upon excitation at 315 nm. Prompt fluorescence is detected at room temperature from isoabsorbing samples; delayed (100 μs after pulse) phosphorescence is registered at 77 K (normalized spectra).

level of the tpy−tpy bridge (the accepting site for the promoted electron consequent to the CT transition) with respect to what happens for the tpy−ph−tpy and $tpy{-}(ph)_2{-}$tpy bridges, as discussed above for the lowest energy absorption features. Actually, this is a well-documented outcome for this type of ligand, ascribed both to the electronic delocalization effect at the ligand itself and to the electrostatic influence exerted by the closer positive metal centers for the case of tpy−tpy as compared to tpy−ph−tpy and $tpy{-}(ph)_2{-}$tpy for a series of Ru(II) dinuclear complexes.[7a] Within the latter series, the better luminescence properties for the smallest size complex (i.e., the one incorporating the tpy−tpy bridge) was explained by the stabilization of the CT emission level, which renders less accessible higher-lying levels of a metal-centered (MC) nature, known to play as doorway to radiationless paths—a recurrent theme for Ru(II)−tpy type emitters.[1,4a] The fact that also, for the present series of Ir(III) dinuclear complexes, a similar trend is registered (Table 3) suggests a role for low-lying energy levels devoid of emission properties (at room temperature (rt)), as we discuss in the following.

For $(dpb)Ir(tpy{-}tpy)Ir(dpb)^{4+}$ at 77 K, the lifetime is τ^{77K} = 2.2 μs, in line with values observed for Ru− and Os−polypyridine CT emitters.[1c,30,31] At this temperature, the emission band maximum moves to higher energy with respect to what happens at 295 K (565 nm vs 620 nm; Figure 2 and Table 3). This is an expected behavior for CT emitters dissolved in polar solvents because on passing from a fluid to a frozen environment, reorientation of the solvent molecules cannot take place, thus hindering stabilization of the CT emission level.[1c]

Comparison of the emission maxima, profiles, and lifetimes for the dinuclear species at 77 K [Figure 2 (lower panel) and Table 3] reveals differences that may be useful to address the nature of the emission for the three dinuclear complexes. First of all, for $(dpb)Ir(tpy{-}ph{-}tpy)Ir(dpb)^{4+}$ (i) the lifetime is τ^{77K} = 5.6 μs (major component; see Table 3) that is again consistent with literature values for CT emitters, and (ii) the band maximum is found to peak at 532 nm, i.e., at higher energy than for $(dpb)Ir(tpy{-}tpy)Ir(dpb)^{4+}$ (562 nm at 77 K). As mentioned above, this is an effect ascribed to insertion of a phenylene group between the two tpy moieties of the bridging ligand, which affects both electronic delocalization and electrostatic factors. For $(dpb)Ir(tpy{-}(ph)_2{-}tpy)Ir(dpb)^{4+}$, the band maximum is registered at 549 nm, i.e., not in line with the expectation of a further blue shift consequent to inclusion of two phenylene groups at the bridging ligand, and the emission lifetime is τ^{77K} = 49 μs (major component, Table 3). Furthermore, the luminescence profile exhibited by $(dpb)Ir(tpy{-}(ph)_2{-}tpy)Ir$-

---

(31) Barigelletti, F.; Ventura, B.; Collin, J.-P.; Kayhanian, R.; Gavina, P.; Sauvage, J.-P. *Eur. J. Inorg. Chem.* **2000**, 113.

(dpb)$^{4+}$ at 77 K appears more structured than for the cases of (dpb)Ir(tpy−tpy)Ir(dpb)$^{4+}$ and (dpb)Ir(tpy−ph−tpy)Ir(dpb)$^{4+}$ (Figure 2). For the 77 K emission of (dpb)Ir(tpy−(ph)$_2$−tpy)Ir(dpb)$^{4+}$, these findings suggest a LC nature.

Figure 3 illustrates luminescence results for the bridging ligands dissolved in dichloromethane, as obtained at room temperature (fluorescence) and at 77 K (phosphorescence), with the latter profiles and lifetimes observed upon introducing a 100 μs delay with the aim of excluding the prompt fluorescence.

Regarding the phosphorescence spectra, along the sequence tpy−tpy, tpy−ph−tpy, and tpy−(ph)$_2$−tpy, a regular bathochromic shift is observed, with $\lambda_{\max}{}^{77\mathrm{K}} = 450$, 507, and 532 nm, respectively, and lifetimes $\tau^{77\mathrm{K}} = 1.17$, 1.49, and 1.44 s, respectively. In particular, one sees that the emission profiles of tpy−(ph)$_2$−tpy and (dpb)Ir(tpy−(ph)$_2$−tpy)Ir(dpb)$^{4+}$ are remarkably similar, with band maxima peaking at 532 and 549 nm, respectively. All of this suggests that for (dpb)Ir(tpy−(ph)$_2$−tpy)Ir(dpb)$^{4+}$, the emission nature at 77 K bears a sizable LC character and, accordingly, should be largely localized at the bridging ligand.

It is interesting that for Ru(II)− and Os(II)−polypyridine complexes characterized by low-lying MLCT levels, a correlation exists between metal-centered oxidation ($E^{\mathrm{ox.}}_{1/2}$) and ligand-centered reduction ($E^{\mathrm{red.}}_{1/2}$) steps, and MLCT absorption and emission peaks. The correlation, which is based on the identification of localized and co-incident orbitals for both redox and spectroscopic data, takes the simplified form of eqs 2,[1]

$$h\nu_{\mathrm{abs}} = a\Delta E_{1/2} + A \tag{2a}$$

$$h\nu_{\mathrm{em}} = b\Delta E_{1/2} + B \tag{2b}$$

$$\Delta E_{1/2} = e(E^{\mathrm{ox.}}_{1/2} - E^{\mathrm{red.}}_{1/2}) \tag{2c}$$

where $h\nu_{\mathrm{abs}}$ and $h\nu_{\mathrm{em}}$ are absorption and emission energies, a and b are linearization parameters, A and B (with $A \neq B$) are empirical terms including electrostatic factors and others, and $\Delta E_{1/2}$ is the so-called "redox energy".[1]

Regarding the here-studied Ir(III) dinuclear complexes, we can notice that (i) the metal-centered oxidation step occurs at very similar potentials in all cases (Table 2) and that (ii) a much positive first reduction step, by ca. 0. 3 V, takes place for (dpb)Ir(tpy−tpy)Ir(dpb)$^{4+}$ with respect to both (dpb)Ir(tpy−ph−tpy)Ir(dpb)$^{4+}$ and (dpb)Ir(tpy−(ph)$_2$−tpy)Ir(dpb)$^{4+}$, and the reference complex (dpb)Ir(tpy−ph(tBu)$_2$)$^{2+}$. For the family of Ir(III) complexes,[25] observation of the metal-centered process is still a rare event and no extended redox data are available in order to test the type of relations of eqs 2. However, the 0.3 V positive ligand-centered reduction step observed for (dpb)Ir(tpy−tpy)Ir(dpb)$^{4+}$ is likely to favor a MLCT nature for the emission, as opposed to the other cases examined here.

Table 4. Transient Absorbance Data, Maximum of the Absorption Band, and Lifetimes

Compound	$\lambda_{\max}$, nm	τ, ps
(dpb)Ir(tpy−ph(tBu)$_2$)$^{2+}$	595	ca. 200 [a]
(dpb)Ir(tpy−tpy)Ir(dpb)$^{4+}$	<500 [a]	>3000 [a]
(dpb)Ir(tpy−ph−tpy)Ir(dpb)$^{4+}$	775	160
(dpb)Ir(tpy−(ph)$_2$−tpy)Ir(dpb)$^{4+}$	780	440

[a] Very weak signal.

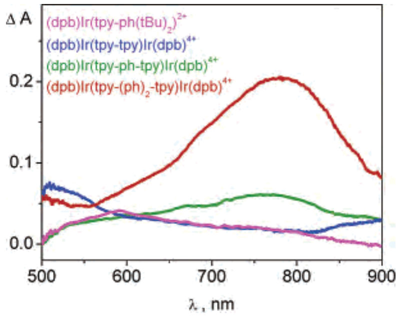

Figure 4. Transient absorption spectra for optically matched ($A = 0.55$) solutions of complexes, registered at the end of the laser pulse (355 nm, 3 mJ/pulse).

Transient Absorption. Transient absorbance (TA) experiments with picosecond resolution and excitation at 355 nm were performed on air-equilibrated samples of the mononuclear and dinuclear complexes (Table 4). These experiments enabled us to detect nonemissive, or scarcely emissive, excited states, and this with a better time resolution than that allowed by our available luminescence equipment. Of course, with TA experiments, one monitors the transitions from the lowest-lying excited state to higher states, whereas the energy of these levels with respect to the ground state can only be derived from luminescence data. The spectra of the mononuclear complex (dpb)Ir(tpy−ph(tBu)$_2$)$^{2+}$, and of the binuclear complexes (dpb)Ir(tpy−tpy)Ir(dpb)$^{4+}$, (dpb)Ir(tpy−ph−tpy)Ir(dpb)$^{4+}$, and (dpb)Ir(tpy−(ph)$_2$−tpy)Ir(dpb)$^{4+}$, detected at the end of a 35 ps pulse are reported in Figure 4.

The latter binuclear complex displays a strong band with maximum at 780 nm which also appears, but with a much lower absorption coefficient in (dpb)Ir(tpy−ph−tpy)Ir(dpb)$^{4+}$ and is absent in (dpb)Ir(tpy−tpy)Ir(dpb)$^{4+}$ and in the mononuclear complex. This indicates a quite different nature in the excited state of the binuclear complex (dpb)Ir(tpy−(ph)$_2$−tpy)Ir(dpb)$^{4+}$ and, in part, of (dpb)Ir(tpy−ph−tpy)Ir(dpb)$^{4+}$ with respect to the other complexes. Nevertheless, a clear assignment as to the nature of the excited state of (dpb)Ir(tpy−(ph)$_2$−tpy)Ir(dpb)$^{4+}$ at 295 K is difficult, since for Ir(tpy)$_2{}^{3+}$ derivatives excited states with both partial LC and CT character have been called for.[9a,28] The decay of the 780 nm band for (dpb)Ir(tpy−ph−tpy)Ir(dpb)$^{4+}$ and (dpb)Ir(tpy−(ph)$_2$−tpy)Ir(dpb)$^{4+}$ can be followed in the time window of the experiment (0−3.3 ns) and lifetimes of 440 and 160 ps are measured, respectively (Figure 5); this fast decay for the excited level of these complexes went undetected by using the available luminescence techniques (see Table 3). The very low absorption of (dpb)Ir(tpy−tpy)Ir(dpb)$^{4+}$ decays only to a modest extent over the ca. 3 ns time window, in agreement with a lifetime of 6.4 ns, as determined by monitoring the luminescence decay (Table 3).

Quite surprisingly, in the mononuclear complex [(dpb)Ir(tpy−ph(tBu)$_2$)$^{2+}$, the weak band peaking at ca. 590 nm decays with a lifetime of ca. 200 ps leaving only a small

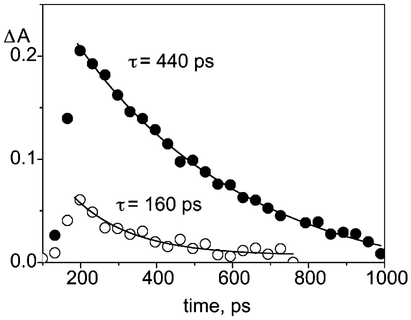

Figure 5. Decay of the absorbance at 780 nm for [(dpb)Ir(tpy−(ph)$_2$−tpy)Ir(dpb)]$^{4+}$ (full circles) and [(dpb)Ir(tpy−ph−tpy)Ir(dpb)]$^{4+}$ (empty circles) with the fitted exponential decays and lifetimes.

residual absorbance at that wavelength. This lifetime is quite different from the one detected on a longer time scale for this complex by luminescence techniques, 3.3 ns (Table 3). A possible explanation for this behavior might be the occurrence of a primary, very fast intramolecular process, subsequently leading to the final emissive state (with τ = 3.3 ns), most likely of LLCT nature.[20,29] Excited-state dynamics between levels of different nature or localization (e.g., LC and LLCT) could be associated to the 200 ps process.

Conclusions

A series of three dinuclear iridium(III) complexes consisting of a conjugated bis-tpy type bridging ligand and cyclometallating capping tridentate ligands of the 1,3-di-2-pyridylbenzene family has been prepared. The electrochemical and spectroscopic properties point to a strong electronic delocalization at the bridging ligand in the first term of the series, the complex (dpb)Ir(tpy−tpy)Ir(dpb)$^{4+}$, whereas for the dinuclear complexes with the longer bridging ligands, (dpb)Ir(tpy−ph−tpy)Ir(dpb)$^{4+}$ and (dpb)Ir(tpy−(ph)$_2$−tpy)-Ir(dpb)$^{4+}$, such an effect is reduced. At room temperature, out of the three complexes, only (dpb)Ir(tpy−tpy)Ir(dpb)$^{4+}$ exhibits an appreciable luminescence. This is ascribed to a larger stabilization of the LUMO level of the tpy−tpy bridge, which is involved in the CT state responsible for the luminescence of (dpb)Ir(tpy−tpy)Ir(dpb)$^{4+}$. For this complex, the CT nature of the excited state is confirmed by the shift of the luminescence profile at higher energy, in passing from room temperature to a rigid glass at 77 K. At this latter temperature, also (dpb)Ir(tpy−ph−tpy)Ir(dpb)$^{4+}$ and (dpb)-Ir(tpy−(ph)$_2$−tpy)Ir(dpb)$^{4+}$ luminesce yet with spectral features similar to those of the phosphorescence of the corresponding free bridging ligands, tpy−ph−tpy, and tpy−(ph)$_2$−tpy, which suggests a sizable LC character for the emission.

At room temperature, the time-resolved absorption spectra found for (dpb)Ir(tpy−(ph)$_2$−tpy)Ir(dpb)$^{4+}$ and, to a lesser extent, for (dpb)Ir(tpy−ph−tpy)Ir(dpb)$^{4+}$ are reminiscent of those previously observed for Ir(tpy)$_2{}^{3+}$ derivatives and do not allow a precise assignment of the excited-state nature. As for (dpb)Ir(tpy−tpy)Ir(dpb)$^{4+}$, the weak absorption detected in the explored wavelength window does not allow speculations with regard to the nature of the excited state, which is however assigned to CT character on the basis of the luminescence results.

Experimental Section

General Procedures. All reactions and manipulations were routinely performed under a dry argon atmosphere. Solvents and chemicals were purchased from commercial sources and used without any purification. Column chromatographies were carried out on silica gel 60 [Merck, 60-200 mesh]. Thin-layer chromatographies (TLCs) were performed on alumina plates coated with silica gel 60 (Merck). ^{1}H NMR spectra were recorded either with Bruker AVANCE 300 (300 MHz), Bruker AVANCE 400 (400 MHz), or Bruker AVANCE 500 (500 MHz). Chemical shifts are indicated in parts per million downfield from SiMe$_4$ using the solvent's peak as internal reference. The numbering schemes of the Ir complexes are given in Scheme 1. Mass spectra were recorded on Bruker MicroTOF instrument (ES-MS). Cyclic voltammetry experiments were performed using an EG&G 273A potentiostat, a Pt working electrode, a Pt counter electrode, a saturated calomel electrode (SCE), 0.1 M Bu$_4$NPF$_6$ as supporting electrolyte, and MeCN as solvent.

Starting Organic Compounds. 1,3-Dipyridyl-4,6-dimethylbenzene was prepared by Stille coupling.[12] The terpyridine tpy−ph-(tBu)$_2$ [9a] and bis-terpyridine tpy−(ph)$_n$−tpy (n = 0,[13] 1,[14] 2 [15]) ligands were synthesized as previously described.

(a) Compound [(dpb)IrCl$_2$]$_2$.[11a] A solution of iridium trichloride (51 mg, 0.17 mmol) and dpbH (44.5 mg, 0.17 mmol) in 2-ethoxyethanol was heated to 80 °C for 3 days. After cooling to room temperature, the brown precipitate was collected, washed with ethanol (3 × 10 mL), and dried under vacuum to give [(dpb)IrCl$_2$]$_2$ as an orange-brown solid (109.2 mg, 61%). ES-MS: 1044.

(b) Compound (dpb)Ir(tpy-ph(tBu)$_2$(PF$_6$)$_2$. A suspension of [(dpb)IrCl$_2$]$_2$ (36.6 mg, 0.035 mmol) and 4′-(3,5-di-*tert*-butylphenyl)terpyridine tpy−ph(tBu)$_2$ (29.5 mg, 0.07 mmol) in ethylene glycol was heated to reflux for 45 min. After cooling to room temperature, the reaction mixture was added to water (7 mL); saturated aqueous solution of KPF$_6$ (7 mL) was then added. The precipitated solid was collected, washed with water (3 × 7 mL), and dissolved in acetonitrile. The brown solid obtained after removal of solvents was purified by silica gel chromatography eluting with a mixture of CH$_3$CN/H$_2$O/(KNO$_3$)$_{sat.}$ (100/3/0.3 to 100/10/1) to give (dpb)Ir(tpy−ph(tBu)$_2$)(PF$_6$)$_2$ as a yellow solid (25.5 mg, 55%). *Rf*: 0.55 (CH$_3$CN/H$_2$O/(KNO$_3$)$_{sat.}$: 100/10/1, SiO$_2$). ^{1}H NMR (300 MHz, acetone-d_6): 9.48 (2H, s, tt$_{3'}$ and tt$_{5'}$); 9.03 (2H, d, J = 8 Hz, tt$_3$); 8.38 (2H, d, J = 8.5 Hz, H$_3$); 8.18 (2H, td, J = 8 and 1.5 Hz, tt$_4$); 8.04 (2H, d, J = 2 Hz, o′); 8.02 (2H, td, J = 8 and 2 Hz, H$_4$); 7.89 (2H,dd, J = 5.5 2 Hz, H$_6$) 7.87 (1H, s, p′); 7.75 (2H, dd, J = 5.5 and 1 Hz, tt$_6$); 7.52 (2H, ddd, J = 5.5, 7 and 1.5 Hz, tt$_5$); 7.46 (1H, s, p); 7.16 (2H, ddd, J = 6, 7.5 and 1.5 Hz, H$_5$); 3.05 (6H, s, Me), 1.52 (18H, s, ^{t}Bu). ^{13}C NMR (100 MHz, CD$_3$CN): 178.5; 170.9; 160.1; 156.1; 154.0; 153.5; 152.4; 141.8; 141.0; 140.9; 138.0; 137.0; 133.7; 129.9; 127.3; 126.5; 125.6; 124.8; 124.6; 124.3; 123.5; 35.9; 31.6; 22.6. HR-ES-MS: 436.6676 ([M − 2PF$_6$]$^{2+}$; C$_{47}$H$_{46}$IrN$_5{}^{2+}$; calcd 436.6687).

(c) Compound (dpb)Ir(tpy−tpy)Ir(dpb)(PF$_6$)$_4$. [(dpb)IrCl$_2$]$_2$ (53.2 mg, 0.05 mmol) and (tpy−tpy) ligand (23.2 mg, 0.05 mmol) were reacted similarly to the above procedure. The brown solid obtained after removal of solvents was purified by silica gel chromatography eluting with a mixture of CH$_3$CN/H$_2$O/(KNO$_3$)$_{sat.}$ (100/3/0.3 to 100/20/2) to give [(dpb)Ir(tpy−tpy)Ir(dpb)] as an orange solid (49.1 mg, 50%). *Rf*: 0.49 (CH$_3$CN/H$_2$O/(KNO$_3$)$_{sat.}$:

100/20/2, SiO_2). ^1H NMR (300 MHz, CD_3CN): 9.51 (4H, s, $tt_{3'}$ and $tt_{5'}$); 8.82 (4H, d, $J = 8$ Hz, tt_3); 8.38 (4H, d, $J = 8.5$ Hz, H_3); 8.18 (4H, td, $J = 8$ and 1.5 Hz, tt_4); 7.92 (4H, td, $J = 8$ and 1.5 Hz, H_4); 7.55 (8H, m, tt_6 and H_6); 7.44 (4H, td, $J = 5.5$ and 1.5 Hz, tt_5); 7.43 (2H, s, p); 7.09 (4H, ddd, $J = 5.5$, 7.5 and 1.5 Hz, H_5); 3.02 (12H, s, Me). ^{13}C NMR (100 MHz, CD_3CN): 177.7, 170.8, 159.6, 156.7, 155.1, 152.4, 150.1, 142.2, 141.4, 140.9, 138.0, 133.7, 130.3, 127.7, 125.7, 125.5, 124.3, 22.6. HR-ES-MS: 342.0868 ($[M - 4PF_6]^{4+}$; $C_{66}H_{50}Ir_2N_{10}{}^{4+}$; calcd 342.0868).

(d) Compound (dpb)Ir(tpy−ph−tpy)Ir(dpb)(PF_6)$_4$. [(dpb)-$IrCl_2$]$_2$ (52.2 mg, 0.05 mmol) and terpyridine−phenyl−terpyridine (27.3 mg, 0.05 mmol) were reacted as described above. The brown solid obtained after removal of solvents was purified by silica gel chromatography eluting with a mixture of $CH_3CN/H_2O/(KNO_3)_{sat.}$ (100/3/0.3 to 100/20/2) to give [(dpb)Ir(tpy−ph−tpy)Ir(dpb)] as a yellow solid (26.2 mg, 26%). *Rf*: 0.17 ($CH_3CN/H_2O/(KNO_3)_{sat.}$: 100/10/1, SiO_2). ^1H NMR (400 MHz, CD_3CN): 9.25 (4H, s, $tt_{3'}$ and $tt_{5'}$); 8.75 (4H, d, $J = 8$ Hz, tt_3), 8.60 (4H, s, o′ and m′); 8.33 (4H, d, $J = 8.5$ Hz, H_3), 8.11 (4H, td, $J = 8$ and 1.0 Hz, tt_4); 7.88 (4H, ddd, $J = 8.5$, 7.5 and 1.5 Hz, H_4); 7.54 (4H, dd, $J = 5.5$ and 1.5 Hz, tt_6); 7.48 (4H, dd, $J = 6.0$ and 1.5 Hz, H_6); 7.37 (2H, s, p); 7.34 (4H, ddd, $J = 5.5$, 8 and 1.5 Hz, tt_5); 7.04 (4H, ddd, $J = 6.0$, 7.5 and 1.5 Hz, H_5); 3.03 (12H, s, Me). ^{13}C NMR (100 MHz, CD_3CN): 178.2; 170.9; 160.1; 156.3; 154.6; 153.5; 152.4; 141.8; 133.7; 141.4; 139.6; 138.0; 130.4; 130.3; 130.0; 127.7; 125.6; 124,8; 124.3; 22.6. HR-ES-MS: 361.0944 ($[M\text{-}4PF_6]^{4+}$; $C_{72}H_{54}Ir_2N_{10}{}^{4+}$; calcd 361.0945).

(e) Compound (dpb)Ir(tpy−(ph)$_2$−tpy)Ir(dpb)(PF_6)$_4$. [(dpb) $IrCl_2$]$_2$ (52.2 mg, 0.05 mmol) and tpy−(ph)$_2$−tpy (30.8 mg, 0.05 mmol) were reacted according to the same synthetic procedure. The brown solid obtained after removal of solvents was purified by silica gel chromatography eluting with a mixture of $CH_3CN/H_2O/(KNO_3)_{sat.}$ (100/3/0.3 to 100/20/2) to give (dpb)(tpy−(ph)$_2$−tpy)Ir(dpb)(PF_6)$_2$ as a yellow solid (27 mg, 25%). *Rf*: 0.20 ($CH_3CN/H_2O/(KNO_3)_{sat.}$: 100/10/1, SiO_2). ^1H NMR (300 MHz, CD_3CN): 9.19 (4H, s, $tt_{3'}$ and $tt_{5'}$); 8.72 (4H, d, $J = 8$ Hz, tt_3), 8.44 (4H, d, $J = 8.5$ Hz, o′); 8.35 (4H, d, $J = 8.5$ Hz, H_3); 8.30 (4H, d, $J = 8.5$ Hz, m′); 8.13 (4H, td, $J = 8.0$ and 2.0 Hz, tt_4), 7.90 (4H, td, $J = 7.5$ and 1.5 Hz, H_4); 7.54 (4H, dd, $J = 6.0$ and 1.0 Hz, H_6); 7.50 (4H, dd, $J = 5.5$ and 1.0 Hz, tt_6); 7.40 (2H, s, p); 7.36 (4H, ddd, $J = 5.5$, 7.5 and 1.5 Hz, tt_5); 7.06 (4H, ddd, $J = 5.5$, 7.5 and 1.5 Hz, H_5); 3.00 (12H, s, Me). ^{13}C NMR (100 MHz, CD_3CN): 178.2; 170.9; 160.1; 156.2; 154.3; 154.0; 152.4; 143.0; 141.8; 141.4; 140.9; 138.0; 137.0; 133.7; 130.1; 129.9; 129.4; 127.3; 125.6; 124.4; 124.3; 22.6. HR-ES-MS: 380.1007 ($[M\text{-}4PF_6]^{4+}$; $C_{78}H_{58}Ir_2N_{10}{}^{4+}$; calcd 380.1024).

Optical Spectroscopy. Spectrophotometric grade acetonitrile or dichloromethane solvents were used. Absorption and luminescence spectra were measured with a Perkin-Elmer Lambda 9 UV−vis−near-IR spectrophotometer and a Spex Fluorolog II spectrofluorimeter, respectively, for air-equilibrated solutions unless otherwise stated. Luminescence quantum yields (ϕ) were evaluated upon excitation of solutions with absorbance < 0.15 at 380 nm (complexes) or 315 nm (ligands), after correction for photomultiplier response, and with reference to air-equilibrated water solutions of $[Ru(bpy)_3]Cl_2$ ($\phi = 0.028$)[32] or acetonitrile solutions of ($[Ir(ttpy)_2](PF_6)_3$ ($\phi = 0.029$)[9a] as standards.[33] Luminescence lifetimes (τ) on the nanosecond or microsecond time scales were obtained with an IBH single photon counting equipment by using pulsed diode sources with excitation at 373 or 278 nm, for complexes and ligands, respectively. For the luminescence spectra and lifetimes in the microsecond-millisecond scale we employed a Perkin-Elmer LS-50B spectrofluorometer equipped with a pulsed xenon lamp with variable repetition rates and time delays; the employed excitation wavelengths are indicated in the text. Transient absorption spectra were determined by a pump−probe spectrograph with 30 ps resolution, based on a Nd:YAG laser (355 nm, 10 Hz).[34] In all cases, elaboration of data was accomplished by using standard programs for fitting mono- or biexponential decays. The experimental uncertainty on the absorption and luminescence maxima is 2 nm; that for the ϕ and τ values is 10%.

Acknowledgment. This research was supported by the CNRS, by CNR Project PM-P03-ISTM-C4/PM-P03-ISOF-M5 (Componenti molecolari e supramolecolari o macromolecolari con proprietà fotoniche ed optoelettroniche), and by FIRB Project RBNE019H9K “Molecular Manipulation for Nanometric Devices” of MIUR. We also thank Johnson Matthey Inc. for a loan of $IrCl_3$.

Supporting Information Available: ^1H NMR spectra and cyclic voltammograms of the three dinuclear iridium complexes. This material is available free of charge via the Internet at http://pubs.acs.org.

IC061009Q

---

(32) Nakamaru, K. *Bull. Chem. Soc. Jpn.* **1982**, *55*, 2697.
(33) Demas, J. N.; Crosby, G. A. *J. Phys. Chem. B* **1971**, *75*, 991.
(34) Flamigni, L.; Armaroli, N.; Barigelletti, F.; Balzani, V.; Collin, J.-P.; Dalbavie, J. O.; Heitz, V.; Sauvage, J.-P. *J. Phys. Chem. B* **1997**, *101*, 5936.